



Original Paper

Mineralogic and Diagenetic Controls on Reservoir Quality of Paleozoic Sandstones, Gebel El-Zeit, North Eastern Desert, Egypt

Bassem S. Nabawy ^{1,4}, Nader T. H. Elgendy,² and Mervat T. Gazia³

Received 20 December 2018; accepted 20 April 2019
Published online: 29 April 2019

Studying the mineral composition and petrophysical properties of the Cambro–Ordovician sequence in Gebel El-Zeit indicates that it can be discriminated into four rock types, namely quartz arenite (RRT1 of the Cambrian Araba Formation, 35 m; RRT2 of the Ordovician Naqus Formation, 320 m), quartz wacke (RRT3) and mudstone (RRT4) of the Naqus Formation. Diagenesis played a major role in reducing or enhancing the studied microfacies. Cementation by silica, compaction and authigenic clay minerals are the main porosity-reducing factors, whereas dissolution and leaching out as well as fracturing are the most important porosity-enhancing factors. For the present study, reservoir quality was determined using reservoir quality index (*RQI*), flow zone indicator (*FZI*) and reservoir potentiality index (*RPI*) based on helium porosity and permeability values, in addition to the mercury injection capillary pressure (MICP) tests. The best reservoir quality was assigned to the quartz arenite microfacies, whereas the least quality was assigned to RRT4. Reservoir quality is mostly controlled by permeability, which in turn is controlled by the helium porosity and the pore radius of the studied samples (r_{35} of Winland and r_{10} of Schowalter). The Araba Formation at the bottom of the sequence is characterized by the best hydraulic flow units (best *RQI*, *FZI*, *RPI* and MICP, rank II). In addition, the middle and top parts of the Naqus Formation have good to very good reservoir quality (rank III).

KEY WORDS: Reservoir quality, Cambro–Ordovician sandstones, Nubia sandstones, Gebel El-Zeit, Diagenesis, Pore structure.

INTRODUCTION

The Gebel El-Zeit area in Egypt is one of the most hydrocarbon prolific provinces in Egypt. It is located on the southwestern onshore of the Gulf of Suez (Fig. 1). In this province, the Paleozoic–Mio-

cene sequences and the basement rocks, reaching total thickness up to 1500 m, are exposed and well represented as NW–SE elongated ridges. The nature of this sedimentary sequence is in part continental, while in other parts marginal, open marine and restricted marine (Allam 1988). The sedimentary sequence is mostly represented by the highly porous and permeable Nubia sandstones as well as the Upper Cretaceous and Miocene sediments. These sediments have been deposited continentally in Gebel El-Zeit but changed into shallow marine in other parts (Allam 1988).

¹Department of Geophysical Sciences, National Research Center, Dokki, Cairo, Egypt.

²Geology Department, Faculty of Science, Tanta University, Tanta, Egypt.

³Mineral Resources Authority, Cairo, Egypt.

⁴To whom correspondence should be addressed; e-mail: bs nabawy@yahoo.co.uk

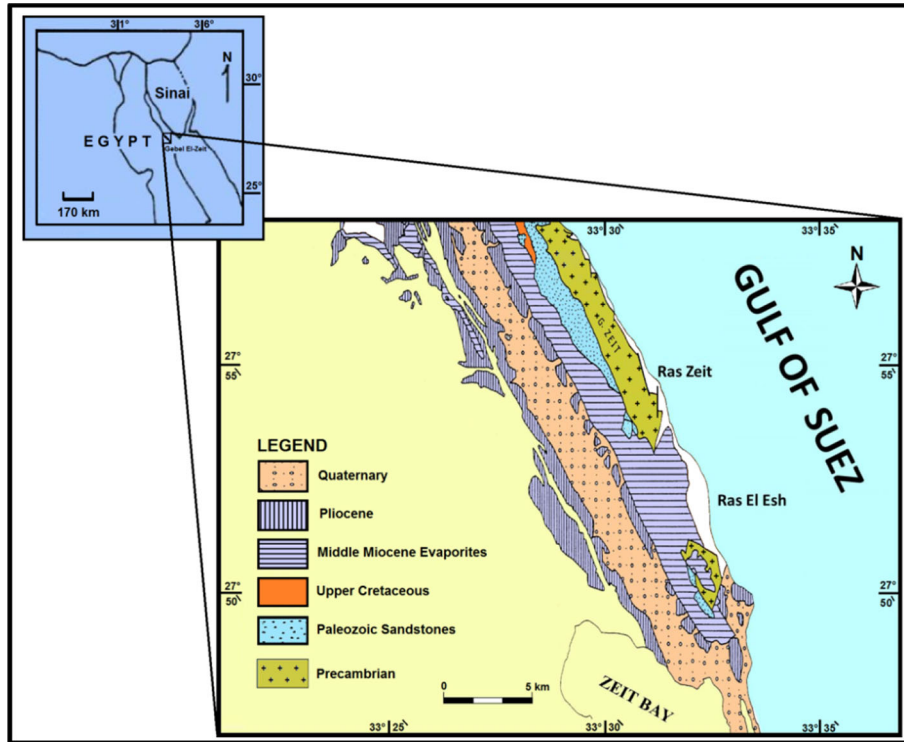


Figure 1. Simplified geological map of the Gebel El-Zeit area showing location of the studied section (Allam 1988).

Gebel El-Zeit ridge extends for 14 km, and it is composed mostly of granites flanked to the west by a 350-m high range of the Paleozoic–Miocene sequence. The Nubia sandstones are among the most prolific sequences in the Gulf of Suez, and their surface exposures in Gebel El-Zeit are a good analog of their subsurface occurrences in the Gulf of Suez. The Nubia sandstones sequence in Gebel El-Zeit is composed mainly of disaggregated to highly cemented clastics with no evaporites and carbonate relics. The sequence is composed of 355 m of fine to coarse-grained quartz arenite with few thin pebbly interbeds. It is divided into Araba and Naqus Formations (e.g., Allam 1988; Abdel-Wahab 1988, 1998). The Paleozoic Nubia sandstone in Gebel El-Zeit is a transitional ridge between the Nubia sandstones occurrences in south Egypt and central Eastern Desert and their occurrences in Sinai and the Gulf of Suez (Nabawy and David 2016; Kassab et al. 2017).

The present study concerns mainly with study of the mineral composition and diagenesis of the Cambrian–Ordovician Araba and Naqus sandstones

in Gebel El-Zeit area to delineate their impacts on the storage and flow capacity as well as the on the reservoir quality Araba and Naqus Formations. The current study has great importance, as it offers an integrated sedimentological and petrophysical studies in Gebel El-Zeit range, which is comparable to the subsurface sequence in the southern province of the Gulf of Suez.

GEOLOGIC SETTING

The exposed sedimentary outcrops in the Gebel El-Zeit area can be divided into 10 rock units; the Cambro–Ordovician Araba and Naqus Formations, the Cretaceous Malha, Galala, Wata and Matulla Formations, and the Miocene Nukhul, Ras El-Bahar, Belayim, South Gharib, and Zeit Formations (Fig. 2). A complex inter-relationship between rifting and sedimentation can be noticed, where a periodic tilting and fracturing of horst blocks with erosional beveling of older deposits following each cycle of sedimentation (Allam 1988).

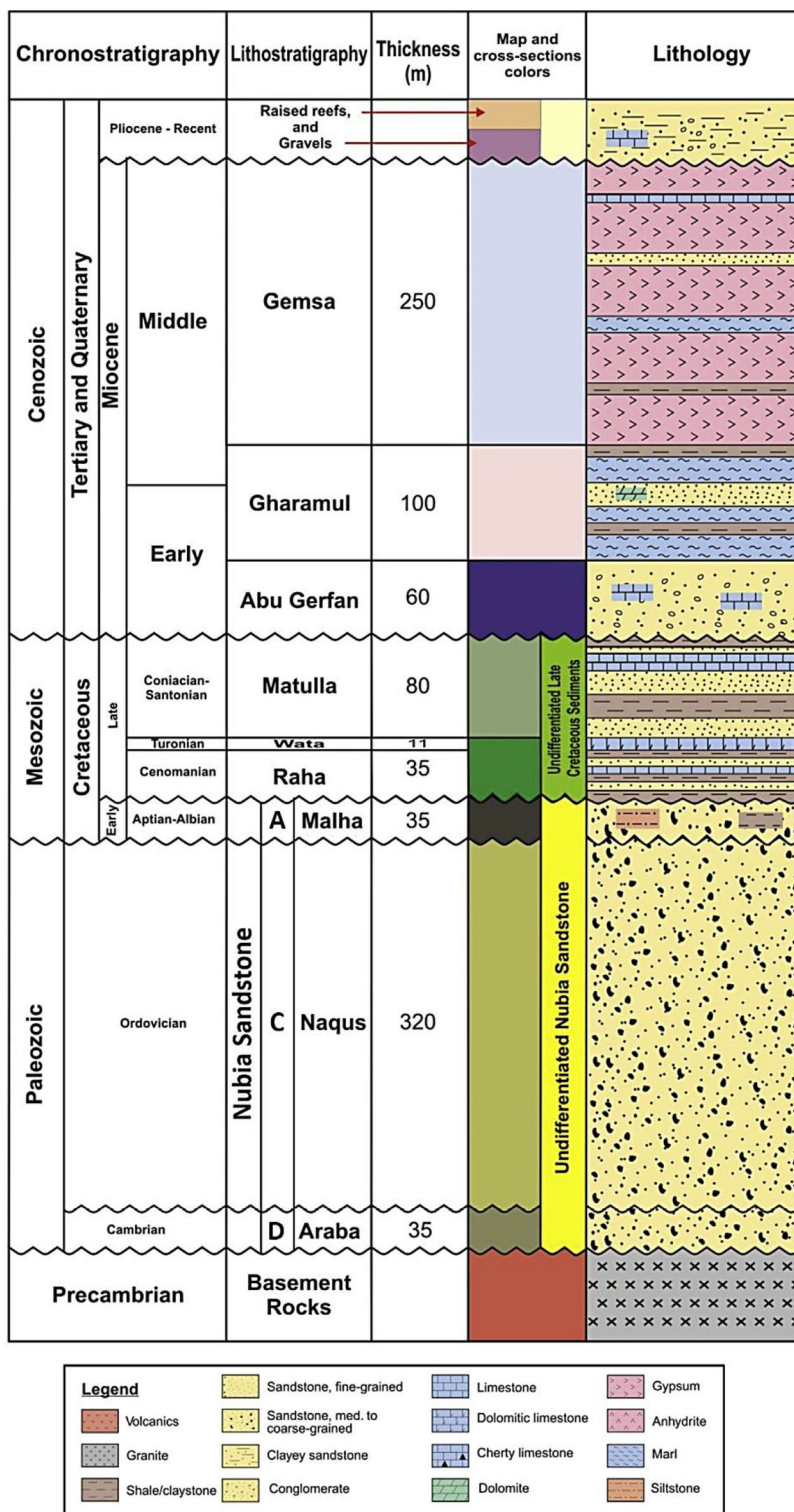


Figure 2. Generalized stratigraphic section of the southern Gulf of Suez (Modified after EGPC 1996; Sakran et al. 2016).

The Araba and Naqus Formations and their coeval units in the Gulf of Suez province have been given various ages, but based on their resting on the Late Pre-Cambrian basement and the local presence of some Skolithos and Stromatolites, they have long been considered as Cambro–Ordovician deposits (Abdallah et al. 1992a, b; Issawi et al. 1999). Some authors tend to assign Cambrian age to the Araba and Naqus Formations, on the western side the Gulf of Suez in particular (Schütz 1994; Ibrahim 1996). Based on the similarity in diagenetic history of these sandstone sequences and the well-documented Carboniferous deposits around the Gulf of Suez, the Early Carboniferous age has been advocated by many authors for these sandstone deposits (e.g., Eames 1984; Ibrahim 1996; Salem et al. 1998).

In the present study, based on field lithostratigraphic relationships, we tend to assign the Cambrian age to the marine Araba Formation in Gebel El-Zeit area. It rests unconformably on the Pre-Cambrian basement rock masses and varies in thickness up to 35 m. Upwards, the Ordovician fluvial Naqus Formation overlies unconformably the Araba Formation on a rough undulated surface with a paleosol layer in places. It is composed of about 320 m of well-sorted laminated, fine- to medium-grained reddish brown cross-bedded sandstone. It contains erratically scattered quartz gravels that are considered as remnants of the Late Ordovician–Early Silurian great Sahara glaciers that covered vast parts of the northwestern parts of Africa (Issawi and Jux 1982; Caputo and Crowell 1985). The unconformity contact between the Araba and Naqus Formations does not represent a hiatus but it is only syn-sedimentary erosion surface due to some changes in sedimentation regime and contemporaneous

changes in the topographic relief (Bhattacharyya and Dunn 1986).

LITHOSTRATIGRAPHY AND DEPOSITIONAL ENVIRONMENTS

The lithostratigraphy of the Paleozoic Nubia sandstone in Gebel El-Zeit is still a matter of controversy due to the lack of guide fossils in the Nubia sandstone. According to the field relationships and to previous studies on the Paleozoic sequence in the western onshore of the Gulf of Suez (Hassan 1967; Allam 1988; Abdel-Wahab 1988, 1998; David et al. 2015; Nabawy and David 2016), the Nubia sandstone sequence in the Gebel El-Zeit area can be distinguished into: (1) Araba Formation (Cambrian) and (2) Naqus Formation (Ordovician).

Araba Formation (35.0 m, Cambrian)

The Araba Formation is composed of 35 m thick of medium- to coarse-grained sandstones dominated by cross-bedding structures. The measured cross-bed sets of the Araba Formation show a current flow direction to the S-SE, suggesting marine transgression from the N-NE. In addition, the Araba Formation wedges out to the south direction, indicating the presence of a highland not far from Gebel El-Zeit. It is mostly barren of fossils and rests directly on the Pre-Cambrian washed granite (Fig. 3a) and underlies unconformably the Naqus Formation. Though there is a problematic confusion about the age of the Araba Formation, the Cambrian age for the Araba Formation is more acceptable among

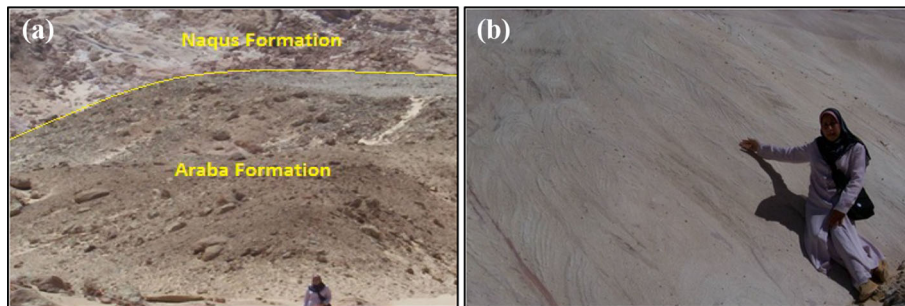


Figure 3. Field photographs showing: (a) contact between the Araba Formation and the overlying Naqus Formation, (b) cross-bedding of medium scale, middle parts of the Naqus Formation.

many authors (e.g., Abdallah and Adindani 1963; Said 1971; Kora 1984; Klitzsch 1986; Beleity et al. 1986; Allam 1988; Khalifa et al. 2006; Gazia 2016).

The basal contact between the Araba Formation and the underlying washed granite is represented by undulatory kaolinitized thin zone containing pebbles and gravels of quartz followed by 10 m of dark red, hard, medium-grained sandstones, sometimes cross-bedded in parts. It is overlain by 5 m of sandy shale to shaly sand of forming excellent flagstone structure and 3 m of gravelly dark brown sandstone. The upper parts of the Araba Formation can be summed up into two main beds described as medium- to coarse-grained reddish sandstones (7 m) with some gravel content aligned as thin beds followed upward by 10 m of reddish, yellowish and violet, fine- to coarse-grained hard cross-bedded sandstone.

Naqus Formation (320 m, Ordovician)

Most authors considered the Naqus Formation as an Ordovician sequence (e.g., Abdallah and Adindani 1963; Said 1971; Kora 1984; Klitzsch 1986; Beleity et al. 1986; Allam 1988; Khalifa et al. 2006). In the Gebel El-Zeit area, the Naqus Formation overlies the vari-colored Araba Formation and underlies unconformably both the Cretaceous sandstones and Carboniferous deposits. It consists of 320 m, mostly well-sorted, subrounded, fine- to medium-grained quartz arenite, sometimes intercalated with shales. Its color ranges from white to various shades of red and purple. Well-rounded quartz pebbles are also found embedded in coarse- to medium-grained sandstone. One of the most diagnostic features of the Naqus Formation is the poorly sorted pebbles and gravels, which are distributed randomly within medium- to coarse-grained, sometimes fine, sandstone. The abundant primary cross-bedding and cross-laminated are additional features that characterize the Naqus Formation (Wanas 2011). These sedimentary features indicate that the Naqus sediments have been transported with a current flow direction of NW to NE from a source area situated to the SE and SW. In addition, its cross-bedding and cross-lamination primary structures indicate deposition in a meandering fluvial environment. The concave-up nature of the trough sets, their high degree of scour, and their parallel laminated beds indicate deposition by relatively high-energy currents and low sinuosity

alluvial system (Allam 1988). The area seems to be affected by the Paleozoic (Caledonian and Hercynian) and Mesozoic movements (Alpine), which led to uplifting the area causing a complete regression followed by transgression of the sea.

The Naqus Formation starts with deposition of 13 m of white to vari-colored, coarse- to medium-grained, cross-bedded sandstones, which are more or less friable and pebbly at the base. It changes upward into vari-colored, coarse-grained, cross-bedded sandstone (22 m). The coarsening upward feature is observed more clearly in the following 55 m of the vari-colored medium- to coarse-grained friable sandstone with gravels. The middle parts of the Naqus Formation consist of 15 m of fine- to medium-grained, friable sandstone topped with a thin bed of reddish brown ferruginous sandy shale (7 m).

The middle parts of the Naqus Formation are characterized by 60 m of vari-colored, medium- to coarse-grained, cross-bedded, friable sand and sandstones with slight pebbly content (Fig. 3b). Upwards, a total thickness of 25.0 m of vari-colored, cross-laminated, medium- to coarse-grained sandstones can be observed (Gazia 2016).

The topmost parts of the Naqus Formation are characterized by vari-colored, medium- to coarse-grained, friable sand and sandstones (52 m) clearly jointed and cross-laminated beds. This sequence represents fluvial deposits (Allam 1988). It is topped by yellowish white, friable sandstones, mostly conglomeratic (Gazia 2016).

Issawi and Jux (1982) considered this formation as a fluvio-glacial sequence deposited by the great Sahara glaciers that invaded vast parts of north-western Africa during the Upper Ordovician–Silurian Period. The presence of some sandstone concretions is more dominant than silts and clays as well as the higher permeability values of the Naqus sandstones permitting easier transport of silica in solution leaving large concretions of spherical and ellipsoidal forms. The formation is formed mostly due to differential and selective weathering.

METHODOLOGY

The geologic setting and lithostratigraphic relationships of both the Araba and Naqus Formations were studied through a number of field trips to Gebel El-Zeit area. A total of 65 surface block samples were selected representatively for Araba (10 block samples) and Naqus (55 block samples)

Formations. The block samples were oriented parallel to the bedding plane. To study the mineral composition and the dominant diagenetic factors, several thin sections were prepared to be studied under a polarized microscope linked to a PC monitor. The thin sections were impregnated with blue dye to describe different types of pore spaces, and stained with Alizarine Red-S to differentiate between dolomite and calcite. In addition, a number of representative rock fragments (20 samples) were studied using scanning electron microscopy (SEM) to scan the pore spaces and to check types and distribution of the different clay minerals. Additional number of representative samples (10 samples) was prepared to define precisely the mineral composition using X-Ray diffraction (XRD).

Petrophysical studies were then applied to plug samples (dried and clean of drilling fluid) obtained representative for each block samples (two plugs, perpendicular and parallel to the bedding plane). To estimate bulk density (σ_b , g/cm³), the studied samples were dried in electric oven at 60 °C for 48 h and then weighed (w_{dry}) using an electronic balance (0.1 mg precision) and bulk volume (v_b) was calculated, where the length and diameters of the plugs were measured using digital micrometer (0.01 mm precision). Several methods were applied to measure porosity and density in the laboratory, where two out of the three volumes [i.e., bulk volume (v_b), interconnected pore volume (v_p), and grain volume (v_g)] must be determined. For the present study, helium injection porosity was determined by measuring the grain volume of the studied samples and then helium porosity was calculated following the procedure introduced by Nabawy and Kassab (2014). Porosity was also estimated using water injection whereby the studied samples were evacuated completely for 2 h using evacuation pump, and then saturated with distilled water. The fully saturated samples were weighed (w_{sat}), and by taking into consideration the dry weight (w_{dry}), the following equation was applied.

$$v_p = (w_{sat} - w_{dry}) / \sigma_w \quad (1)$$

$$\phi (\%) = 100 \times (v_p / v_b) = 100 \times (w_{sat} - w_{dry}) / v_b \quad (2)$$

where v_p is the total pore volume.

Permeability (k) values were measured using nitrogen gas permeameter, whereby the samples were introduced into a Hassler-type core holder and

permeability was measured for the vertical and horizontal plug samples (k_H and k_V) following Nabawy and Kassab (2014), Nabawy (2015).

For reservoir quality discrimination, the concept of hydraulic flow units was used. This concept is based on reservoir quality parameters including reservoir quality index (RQI , μm), normalized porosity index (NPI , 0.00) and flow zone indicator (FZI , μm) to discriminate a reservoir into rock types and flow units (Amaefule et al. 1993; Kassab et al. 2017; Lai et al. 2015, 2016; El Sharawy and Nabawy 2016a; Nabawy and Barakat 2017; Nabawy et al. 2018). FZI was calculated using the following equation.

$$FZI = RQI / NPI \\ = \left(0.0314 \times (k/\phi)^{1/2} \right) / (\phi / (1 - \phi)) \quad (3)$$

where k is measured permeability (md) and ϕ is porosity (0.00).

For the present study, to get more representative reservoir quality, we calculated the RQI and FZI using the geometric average of permeability not traditionally based on the horizontal permeability as advised by Nabawy (2015) for carbonate rocks. The reservoir potential index (RPI , 0.00) is additional parameter introduced by Nabawy and Al-Azazi (2015) and modified by Nabawy et al. (2018) for ranking reservoir quality to avoid discordance between the ranks introduced from both RQI and FZI ranking parameters.

$$RPI = (RQI_{rank} + FZI_{rank}) / 2 \quad (4)$$

The pore throat distribution was estimated using mercury injection capillary pressure (MICP) technique at pressures ranging from 1 up to 30,000 psi for a total of 28 samples (5 samples from the Araba Formation, 23 samples for the different facies of the Naqus Formation), whereby the progressive increment of the applied pressure is accompanied by a progressive increment of the mercury invasion inside narrower pore spaces. Therefore, the higher the applied pressure, the smaller the pore throat radius invaded (Nabawy and Barakat 2017). From the MICP plots, r_{35} and r_{dp} can be defined as useful tools for studying the main permeability-controlling factors, and for characterizing the pore throat diameters and distribution as well. Following Winland (1972), r_{35} of a given rock sample is calculated as the corresponding pore throat radius at 35% of mercury saturation (Kolodzie 1980; Pittman 1992;

Spearing et al. 2001; Nabawy and Barakat 2017). The displacement pressure (r_{dp}) is pressure required to displace fluids inside the pore spaces or it is pressure at which the first fluid filament was created. It can be estimated from the applied pressure-mercury saturation plot as described by many authors (Schowalter 1979; Katz and Thompson 1987; Nabawy and Barakat 2017; Nabawy et al. 2018).

RESULTS OF MICROFACIES ANALYSIS

Petrographic Studies

The mineral composition of the studied Cambro–Ordovician Araba and Naqus samples indicates the presence of three microfacies: (1) quartz arenite, (2) quartz wacke, and (3) mudstone (Gazia 2016). Each microfacies has distinctive aspects that are visible and identifiable under the microscope.

Quartz Arenite Microfacies

In Araba Formation, this microfacies is represented by cross-bedded, friable to hard, ill-sorted, fine- to coarse-grained sandstones. It represents the base and top parts of the Naqus Formation; it is represented by the cross-bedded, vari-colored, hard to friable, ill-sorted, medium- to coarse-grained, sometimes pebbly, sandstones (Fig. 3b).

Petrographically, the quartz arenite facies is composed of ill-sorted, very fine to coarse, angular to subangular quartz grains cemented with silica cement as pressure solution. The quartz grains are in contact with each other with different grades; point contact, concave–convex contact, and suture contacts (Fig. 4a and b). The grains are dominantly monocrystalline, rarely polycrystalline, with wavy extinction (Fig. 4a). Some few dark patches of clay minerals are presented filling the pore spaces and masking the borders of the grains (Fig. 4a).

The estimated porosity values of the studied microfacies in both the Araba and Naqus Formations are good to excellent and ranges between 15 and 29. The studied pore spaces can be grouped into: (1) inter-granular porosity (Fig. 4a and b), and (2) microfracture porosity (Fig. 4a).

Quartz Wacke Microfacies

The quartz wacke is widely distributed in the Naqus Formation. It is composed mostly of fine- to medium-grained sandstones, friable to moderately hard, and slightly pebbly to gravely sandstone. The beds of this facies are mostly cross-laminated and sometimes cross-bedded.

Petrographically, it is composed of very fine- to coarse-grained, angular to rounded, sometimes are polycrystalline, quartz grains. The cement is composed mainly of silica besides some gypsum and clay patches (Fig. 4c). The grains are compacted together in point, suture and concave–convex contacts. Some clay and gypsum patches (17.9–48.1%) are present as matrix/cement, and sometimes as pore filling. Porosity of the studied rocks of this facies is good to very good (16–23%) and can be distinguished as: (1) inter-granular porosity; partially reduced by gypsum and clay content (Fig. 4c), and (2) microfracture porosity.

Mudstone Microfacies (Siltstone)

The mudstone microfacies is mostly represented in the topmost parts of the Naqus Formation. It is represented by vari-colored, cross-laminated, very fine sandstones and siltstone. Petrographically, this facies is composed of highly compacted, moderately to well-sorted, very fine to silty-sized angular quartz grains (23.5–25.9%) float and embedded in clay matrix (73.4–76.1%) and gypsum cement with more or less parallel lamination (Fig. 4d).

Porosity of the mudstone microfacies is poor to fair; it does not exceed 12% and represented by: (1) microinter-granular porosity, (2) matrix porosity (Fig. 4d), and (3) meso- to macrochannel porosity (Fig. 4d).

Scanning Electron Microscope (SEM) Studies

The SEM helped greatly in studying the pore spaces and the factors controlling the pore volume evolution. In the Araba samples, the interstitial pore spaces are represented by inter-granular pore spaces, sometimes are reduced by some clay min-

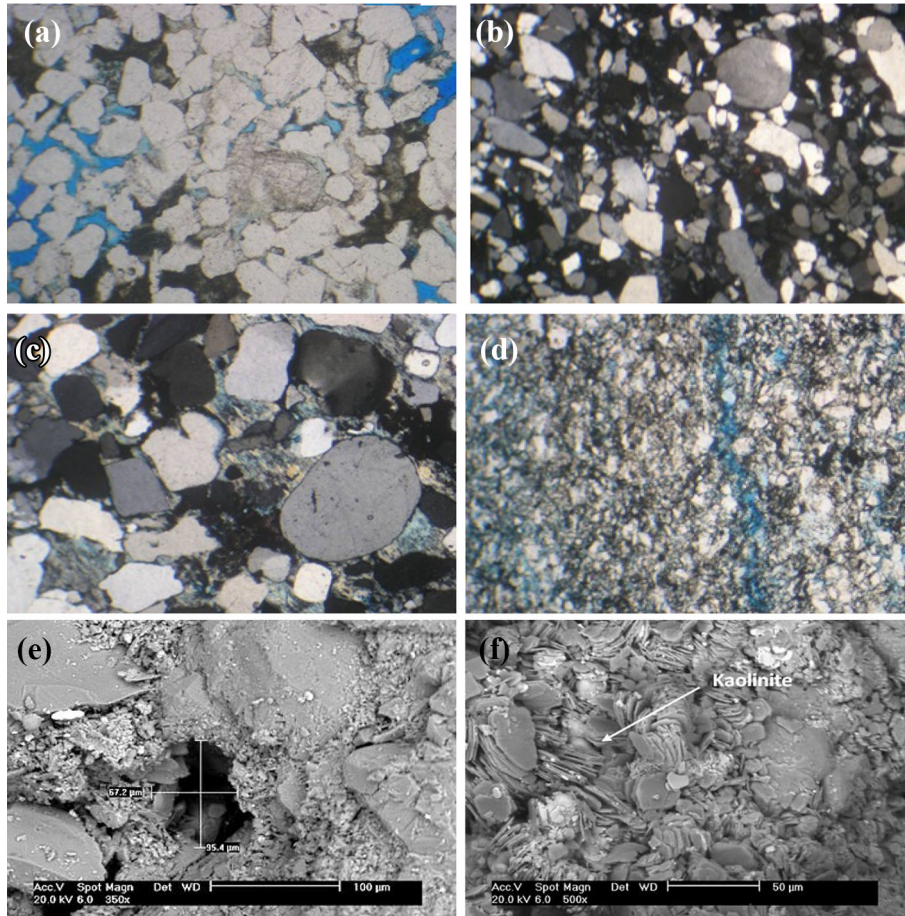


Figure 4. Photomicrographs showing; (a) angular compacted grains with some dull clay patches filling the pore spaces, quartz arenite microfacies, Araba Formation, PPL, 40X; (b) very fine to coarse-grained compacted together with some orientation, quartz arenite microfacies, Naqus Formation, C.N, 40X; (c) moderately sorted fine to coarse quartz grains with poor inter-granular porosity due to filling by gypsum needles, quartz wacke microfacies, Naqus Formation, C.N, 40X; (d) silt-sized quartz grains with clay content filling the pore spaces with some meso- to macrofracture porosity, mudstone microfacies, Naqus Formation, PPL, 10X. SEM Photomicrographs showing; (e) macro- (size $\geq 75.0 \mu\text{m}$) to meso ($75.0 \mu\text{m} \geq \text{size} \geq 30.0 \mu\text{m}$) pore spaces reduced by clays, quartz arenite microfacies, Araba Formation; (f) macrointer-granular porosity filled with well-developed kaolinite booklets, quartz wacke microfacies, Naqus Formation.

erals (Fig. 4e). In some samples, porosity is represented by fracture porosity rarely reduced by gypsum laminae. The pore spaces are mostly macro- to mega-inter-granular pore spaces (Fig. 4e). The pore spaces of the Naqus Formation are mostly inter-granular and fracture pore spaces and sometimes are reduced by well-developed kaolinite booklets and gypsum laminae (Fig. 4f). The kaolinite clay content is well developed than in the Araba Formation giving rise to quartz wacke microfacies. The pore spaces are mostly macro- to meso-inter-granular pore spaces, sometimes these pore spaces are of macro- to meso-size inter-granular and vuggy pores

(Fig. 4f). Upwards, through the Naqus Formation, the percentage of clay content and gypsum laminae increases with decreasing quartz content, where the mudstone microfacies forms a good thickness through the top of the formation (Gazia 2016).

X-ray Diffraction 'XRD' Studies

The XRD analyses indicate that the quartz arenite of the Araba and Naqus samples are composed mainly of quartz, which constitutes the main component ($85\% \leq \text{quartz} \leq 99\%$). The other

Table 1. XRD analysis of samples from the studied Araba and Naqus Formations

Formation	Sample no.	Quartz SiO ₂ (%)	Kaolinite Al ₂ Si ₂ O ₅ (OH) ₄ (%)	Gypsum CaSO ₄ ·2H ₂ O (%)	Montmorillonite (Na,Ca) _{0.33} (Al,Mg) ₂ Si ₄ O ₁₀ (OH) ₂ ·n(H ₂ O) (%)
Araba Formation	1	96	–	4	–
	2	92	5	3	–
	3	88	8	4	–
	4	97	2	1	–
	5	99	1	–	–
Naqus Formation	1	94	6	–	–
	2	75	12	13	–
	3	54	22	24	–
	4	66	15	19	–
	5	78	22	–	–
	6	82	16	2	–
	7	85	12	3	–
	8	91	7	–	2
	9	91	8	–	1
	10	90	9	–	1
	11	78	22	–	–
	12	26	74	–	–

constituents are mostly represented by kaolinite (0–12%) and gypsum of not more than 4% (Table 1). Upwards in Naqus Formation, the quartz arenite is sometimes rich in gypsum; it may reach up to 24%. Some traces of montmorillonite are rarely recorded in the Naqus samples component (1%, Fig. 5 and Table 1) (Gazia 2016).

The quartz wacke samples are composed of quartz (54% ≤ quartz ≤ 78%) and kaolinite (22%) as main components. In some samples, gypsum is present as a main component (24%, Table 1, Fig. 5). The higher ratios of kaolinite in the quartz wacke samples may be attributed to precursor feldspars that have been disintegrated into kaolinite. The mudstone microfacies is represented by sample no. 30, where the main components are kaolinite (64%) and quartz (36%, Table 1 and Fig. 5).

Diagenetic Factors Controlling the Pore Volume

Diagenetic factors exert an intensive control on reservoir quality and on homogeneity or heterogeneity (Morad et al. 2010). So, a detailed study determines influence of dominant diagenetic factors on reservoir quality is of major importance to characterize hydrocarbon reservoirs and for further hydrocarbon exploration. Diagenetic factors, including compaction, cementation, fracturing, dissolution and leaching out, and formation of authigenic minerals (e.g., pyrite and clay minerals),

control the formation and distribution of good hydraulic flow units in a reservoir sequence (Lai et al. 2018b). This is due to their effect on the composition and texture of sedimentary rocks, i.e., due to their enhancing or reducing impacts on pore volume, fluid flow efficiency, and petrophysical potentiality of the studied samples.

Nabway and Kassab (2014) mentioned that dissolution and leaching out as well as fracturing are the most important porosity-enhancing processes, while cementation, compaction, pressure solution, authigenic minerals, and aggrading neomorphism are the most important porosity-reducing diagenetic processes.

Mechanical compaction, cementation by calcite and silica, and formation of diagenetic minerals have a major role in reducing the primary inter-granular pore spaces, whereas dissolution of cement and unstable grains act as a positive factor to enhance of reservoir quality (Lai et al. 2017b).

The main diagenetic factors controlling the petrophysical reservoir quality evolution of the studied samples are summed up into two groups as follows.

Porosity-Reducing Diagenetic Processes

The porosity and reservoir quality-reducing diagenetic factors are mostly formed as eogenetic and mesogenetic diagenesis, where mechanical

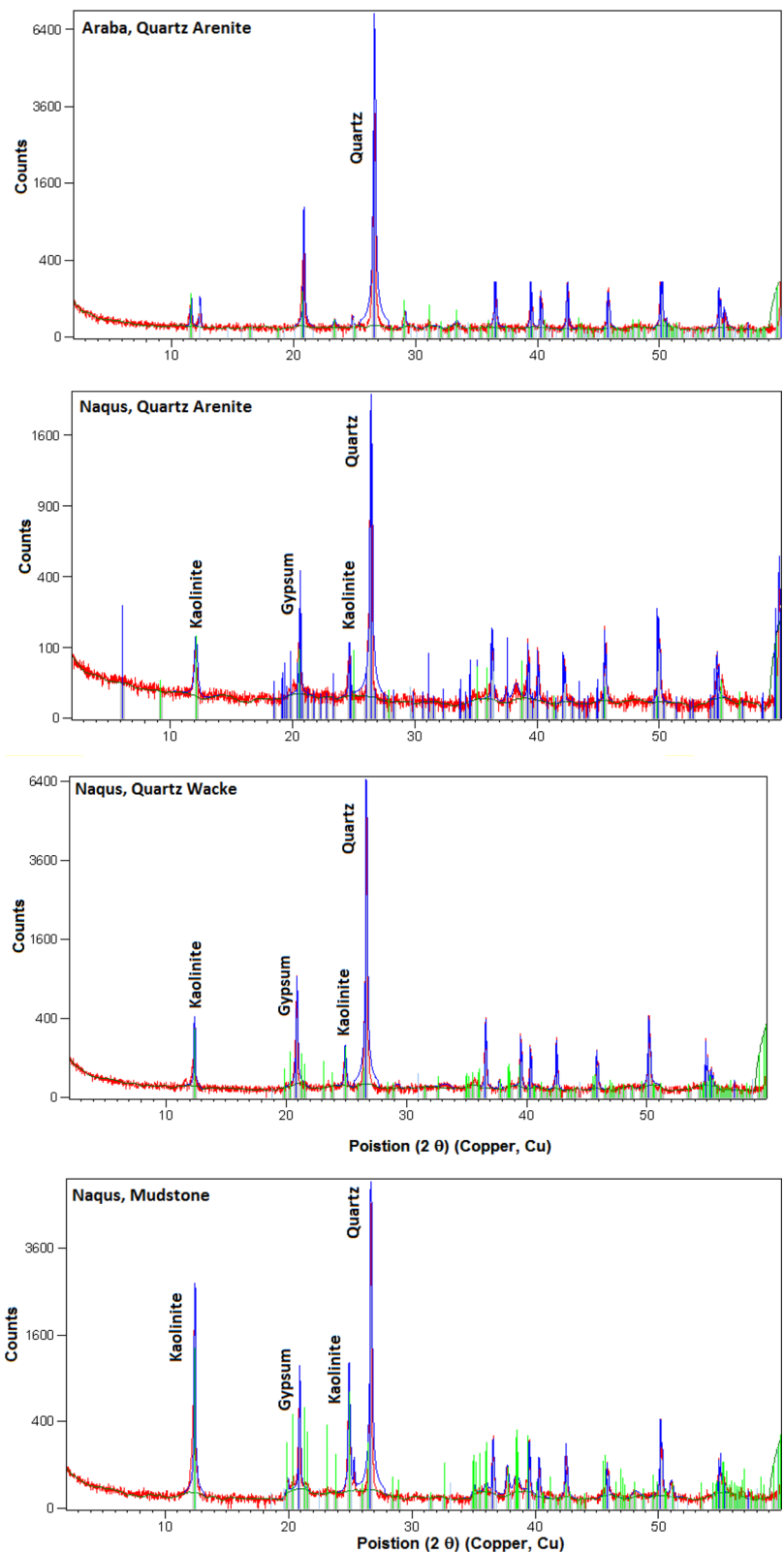


Figure 5. X-ray diagrams for the bulk samples of the studied microfacies, the Araba and Naqus Formations, Gebel El-Zeit.

compaction and quartz overgrowth are considered as eogenetic diagenetic stage. Subsequent alteration of feldspars and precipitation of silica cement and authigenic clay minerals are considered as mesogenetic diagenetic stage.

Mechanical Compaction Increasing mechanical compaction by increasing overload pressure with depth in the eogenetic diagenetic stage is one of the eodiagenetic processes, which are responsible for loss of pore volume with time progress. The Nubia sandstone in Gebel El-Zeit underwent mechanical compaction relatively sufficient to develop sutured quartz grain contacts (Fig. 4b), concave-convex (Fig. 4c) and point contact, and reduced porosity down to 15% in some samples of both the Araba and Naqus Formations. The compaction was not high enough to occlude the pore volume; it was suitable for releasing meniscus and pressure solution silica, less than 8%. Progressive compaction of the Araba and Naqus Formations led to wavy extinction in some quartz grains and fracturing in other quartz grains.

Cementation Cementation as mesogenetic diagenetic factor is the main porosity-reducing factor that causes blocking and reduction of pore volume with progressive cementation and pore filling. For the studied samples, silica is the main dominant cement, which is represented as meniscus texture. It is mostly due to pressure solutions and compaction of quartz grains, which caused suture and concave-convex texture and partial dissolution of quartz borders followed by cementation of quartz grains in the quartz arenite microfacies of the Araba and Naqus Formations (Fig. 4a and b) and the quartz wacke microfacies of the Naqus Formation. The absence of calcite cementation may be attributed to early burial during the diagenetic history with introducing some quartz meniscus cement, which halted the calcite cementation. Another explanation for the absence of calcite cement may be attributed to intensive dissolution and leaching out of this subsidiary cement and oxidation by oxidizing meteoric water to replace the calcite by gypsum cement. The gypsum laminae are mostly noticed in the Naqus Formation in the quartz wacke microfacies where it may reach up to 24% as indicated from the XRD analysis (Table 1). It is presented as laminae, in which the grains are flowing in a poikilotopic texture of gypsum (Fig. 4c) cemented the grains together, and filling the fractures (Fig. 4e) and the inter-granular pore spaces as well. Downward in Araba Formation, gypsum is found as minor filling

constituents, does not exceed 4% as stated from the XRD data (Table 1), reducing the inter-granular pore spaces and fractures.

Authigenic Minerals Kaolinite, the most common authigenic mineral in the studied samples, has been formed during the mesogenetic diagenetic stage; it is indicated petrographically as dull patches filling the interstitial pore spaces in the quartz arenite microfacies of the Araba and Naqus Formations (Fig. 4a). The percentage of kaolinite increases in the quartz wacke microfacies of the Naqus Formation up to 22% (Fig. 4c) and reaches its highest percentage (74%) in the mudstone microfacies (Fig. 4d) as indicated from XRD data, which ensured that the detected dull patches are kaolinite clay minerals (Table 1). The present kaolinite content greatly reduced the effective pore volume, particularly in the mudstone microfacies, where it is present as authigenic clay minerals filling and reducing the inter-granular porosity of the quartz arenite microfacies of the Araba and Naqus Formations (Fig. 4e), and the quartz wacke microfacies of the Naqus Formation (Fig. 4f) and the mudstone microfacies of the Naqus Formation as shown from the SEM studies.

Porosity-Enhancing Diagenetic Processes

Dissolution and Leaching Out Dissolution and leaching out of the rock framework due to invasion of meteoric water during teleodiagenesis are considered the most important porosity-enhancing diagenetic factors of the studied samples. This process has the most intensive effect throughout the different microfacies of the Araba and Naqus Formations with the exception of the mudstone microfacies near top of the Naqus Formation where its effect is relatively low. Deposition of the quartz sandstones of the present Cambro-Ordovician Formations seem to be characterized by very high porosity but followed by local calcite cementation, which prohibited the progress of intensive compaction process from controlling the diagenetic history of the studied samples. This calcite cementation, however, seems to be followed by severe dissolution of the carbonate cement and the feldspars, which is attributed to later extensive invasion by oxidizing meteoric water. The dissolution and leaching out of calcite cement by low Ca-bearing solutions can be indicated by the absence of carbonate cement, which is present as trace precursors in few samples. The dissolution of feldspars

is indicated by accumulations of some kaolinite content as authigenic booklets filling the pore spaces as shown in the quartz arenite microfacies, the quartz wacke (Fig. 4f) and the mudstone microfacies of the Naqus Formation. Dissolution and leaching out by the dissolving solutions in both the Araba and Naqus Formations enhanced the fracture systems into channels system and lead to evolution of excellent inter-granular porosity (Fig. 4e), meso- to mega-vuggy porosity (Fig. 4c and e), and sometimes intra-granular porosity.

Fracturing Petrographically, fractures introduced the main pathway for dissolving solution, to dissolve and leach out the precursor carbonate cement and the feldspars content. On microscale, rare micro- to mesofractures are noticed through the main groundmass of the quartz arenite microfacies and the mudstone microfacies (Fig. 4d) of both the Araba and Naqus Formations.

PETROPHYSICAL RESULTS

The studied Cambro–Ordovician microfacies are characterized by good to very good petrophysical potential ranks (Table 2). The petrographic and petrophysical properties of the pore and petro-phases of the studied microfacies are critical key factors for reservoir rock typing (RRT) into four RRTs. The best potential rank is assigned to the quartz arenite in both the Araba and Naqus Formations, which can be discriminated from each other into two rock types (RRT1 and RRT2) based on their petrophysical values. The least potential rank is assigned to the mudstone microfacies (RRT4) of the Naqus Formation, whereas the quartz wacke microfacies is a transitional petrophysical facies (RRT3) among the different rock types (Table 2).

Porosity (ϕ_{He}) varies from 6.99% for RRT4 mudstone samples up to 28.2% for RRT2 quartz arenite samples of the Naqus Formation, whereas the best permeability value (2196 md) is assigned to RRT1 of the Araba Formation and the least value is 0.09 md for RRT4 samples (Table 2). The pore throat distribution of RRT2 samples is ranked II on average, RRT1 samples as rank III, whereas mudstone RRT4 samples as rank V.

A set of bivariate relationships and statistical models are introduced to model the inter-relationship between the different petrophysical parameters and to be applied for further prediction of petrophysical parameters in terms of others.

Table 2. Pore and Petro-phase storage capacity, electric properties and reservoir quality parameters of the studied microfacies in the Gebel El-Zeit area

Formation	Lithology	σ_g (g/cm ³)	σ_b (g/cm ³)	ϕ_{He} (%)	ϕ_w (%)	ϕ_{inacc} (%)	k_H (md)	k_{av} (md)	k_V (md)	RQI (μm)	FZI (μm)	RPI (0.00)	r_{35} (μm)	r_{dp} (fm)	MICP (rank)
Araba Formation	RRT1 (Quartz Arenite)	Min	2.641	2.074	15.9	11.9	5.29	650	577	468	1.89	3.00	10.52	13.86	III
	Average		2.655	2.153	18.9	15.9	16.0	1633	1424	1070	2.69	4.00	14.39	18.74	III
	Max		2.678	2.239	21.7	20.4	25.1	3118	2224	1876	3.32	4.00	17.65	22.30	II
Naqus Formation	RRT2 (Quartz Arenite)	Min	2.511	1.835	20.1	17.1	6.27	489	498	445	1.44	3.00	12.36	17.85	III
	Average		2.565	1.944	24.2	21.1	13.0	1268	1157	1059	2.16	3.00	18.79	24.03	II
	Max		2.635	2.056	28.2	24.9	21.1	2699	2166	1869	2.91	3.00	27.28	35.96	II
RRT3 (Quartz Wacke)	Min	2.569	2.089	14.2	9.23	11.5	26.2	43.9	32.4	0.54	2.98	2.00	2.38	3.78	V
	Average		2.606	2.161	17.1	12.6	26.2	310.4	294.9	291	1.13	2.00	4.82	8.48	IV
	Max		2.637	2.245	20.2	16.5	38.3	965.3	1268	1932	2.59	4.00	11.15	18.53	IV
RRT4 (Mudstone)	Min	2.600	2.325	6.99	1.17	42.3	0.17	0.09	0.04	0.03	0.31	0.00	0.13	0.21	V
	Average		2.633	2.378	9.70	3.70	62.9	0.63	0.39	0.05	0.53	0.00	0.15	0.31	V
	Max		2.658	2.445	12.2	6.06	83.3	1.67	1.00	0.08	0.83	0.00	0.18	0.46	V

σ_g and σ_b are bulk and grain densities, respectively; ϕ_{He} and ϕ_w are porosity values measured by the helium and water injection techniques, respectively; ϕ_{inacc} is porosity that is inaccessible by water injection; k_H , k_{av} and k_V are the horizontal, average and vertical corrected permeability, respectively; RQI and FZI are reservoir quality index and flow zone indicator, respectively (Amaefule et al. 1993); RPI is reservoir potential index (Nabawy and Al-Azazi 2015); r_{35} is pore radius introduced by Winland (1972) that corresponds to 35% mercury saturation; r_{dp} is pore radius corresponding to the displacement pressure as described by Schowalter (1979); and MICP rank is reservoir rank assigned based on mercury injection capillary pressure plots

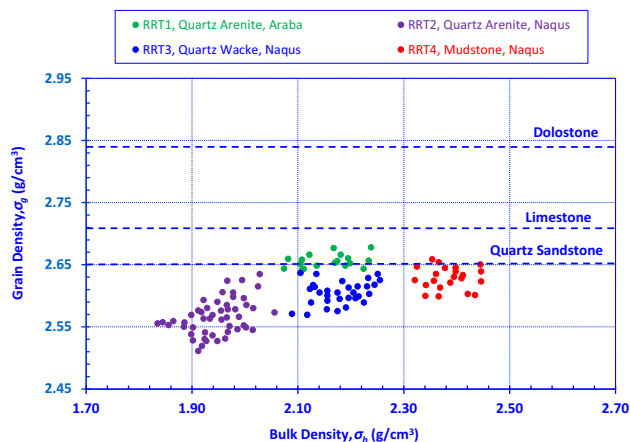


Figure 6. Plots of grain density (σ_g) as a function of bulk density (σ_b) as a tool for lithology determination for the studied samples.

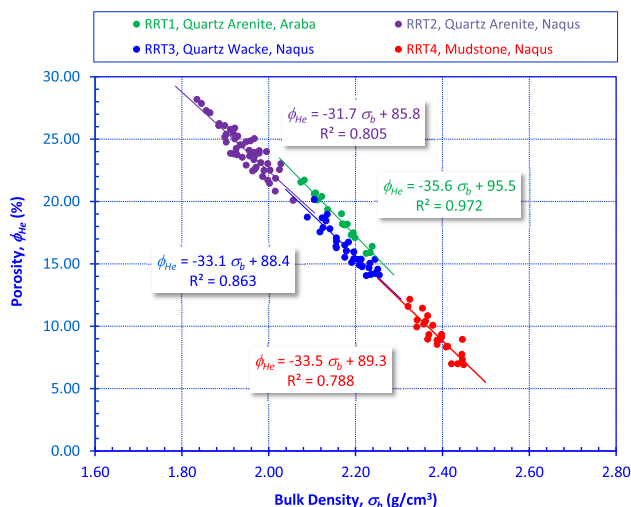


Figure 7. Plots of bulk density (σ_b) vs. porosity measured by helium injection (ϕ_{He}), Paleozoic Nubia sandstones, north Eastern Desert, Egypt.

Lithology Discrimination

Plotting grain density (σ_g) as a function of bulk density (σ_b) is recommended to assign the different lithologies based on petrophysical data. Petrographical description must be taken into consideration (Kassab et al. 2017). Scattering of bulk density data with respect to x -axis of the $\sigma_g - \sigma_b$ ($1.835 \text{ g/cm}^3 \leq \sigma_b \leq 2.623 \text{ g/cm}^3$) plot indicates heterogeneity in the pore volume distribution through the different samples (Fig. 6). Weak heterogeneity is noted for grain densities indicating quartz arenite ($\sigma_g \approx 2.65 \text{ g/cm}^3$) to mudstone facies, where the

grain density is mostly less than 2.65 g/cm^3 . The quartz arenite microfacies in both the Araba and Naqus Formations can be easily distinguished on this plot with much less grain and bulk densities for the Naqus Formation. This relatively low grain density for the quartz arenite of the Naqus Formation ($2.511 \text{ g/cm}^3 \leq \sigma_g \leq 2.635 \text{ g/cm}^3$) can be attributed to the presence of some completely isolated pore spaces that reduce the sample weight but do not affect the grain volume (Nabawy and Wassif 2017). The relatively low bulk densities indicate relatively higher and very good porosities.

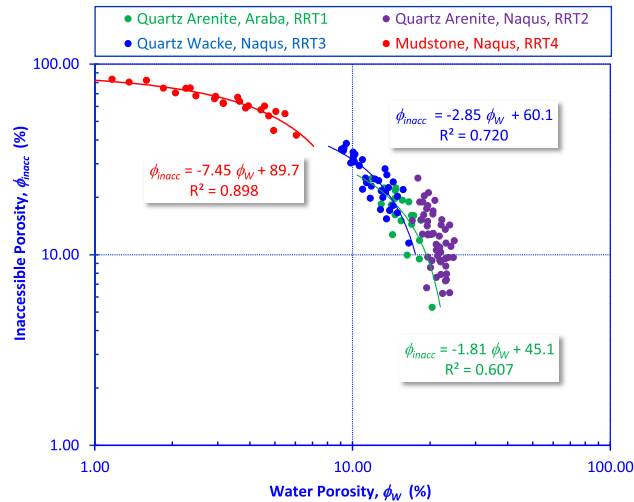


Figure 8. Plots of inaccessible porosity (ϕ_{inacc}) as a function of the water porosity (ϕ_w).

Quality Control for the Studied Samples

Plotting bulk density as a function of porosity (Fig. 7) can be applied as a quality control for the processed data before further processing and modeling (El Sharawy and Nabawy 2016b; Kassab et al. 2017). The relatively high coefficients of determination ($0.972 \geq R^2 \geq 0.788$, Fig. 7) for the different rock types indicate the reliability and consistency of the measured data and their suitability for further statistical processing.

The difference between porosities measured by helium and water is referred mostly as inaccessible porosity (ϕ_{inacc} , %) and can be attributed to the fact that helium gas can invade the micro- and nanopore spaces down to 50 nm, which are not accessible by injected water. It can be calculated as the ratio of the difference between the helium and water porosities thus:

$$\phi_{inacc} = 100 \times (1 - \phi_w / \phi_{He}) \quad (5)$$

The ratio reaches up to 25.1% for the quartz arenite facies (RRT1, RRT2), up to 38.3% for the quartz wacke (RRT3) and up to 83.3% for the mudstone microfacies (RRT4, Table 2). This water-inaccessible micro- and nanopore spaces are referred as to impervious and poor hydraulic flow units (Nabawy and El Sharawy 2015; El Sharawy and Nabawy 2016a; Nabawy et al. 2018). The inaccessible porosity has mostly reliable empirical inversely proportional relationship with water porosity ($R^2 \geq 0.607$, Fig. 8), except for the quartz arenite in

the Naqus Formation ($R^2 = 0.331$) indicating heterogeneity in distribution of this portion from one sample to another. The inaccessible porosity can be calculated in terms of water porosity of different rock types using the following empirical equation

$$\phi_{inacc} = -2.75\phi_w + 66.5 \quad (R^2 = 0.849) \quad (6)$$

GENERAL DISCUSSION

The net result of the petrophysical behavior and the reservoir quality is mostly the contribution of the mineral composition, the pore and petro-fabrics and the diagenetic controlling factors. In addition, the flow capacity of the rock sequences is the main contribution of the storage capacity and pore types. These controlling key factors and their impacts on the reservoir quality properties of the Cambrian-Ordovician Arab and Naqus Formations are discussed in the following section.

Impacts of Diagenesis on Petrophysical Properties

Heterogeneity or homogeneity of clastic reservoirs determines the net pay thickness, the flow regimes and rates, and hydrocarbon production. Heterogeneity of sandstone reservoirs is mostly controlled by geometry and structures of the sand beds, lobes and lenses, grain size and sorting as

primary factors in addition to types, intensity, and distribution of diagenetic processes. The distribution and pathways of diagenetic processes are mostly governed by (1) mineral composition, (2) porosity and permeability, amounts, types and mode of distribution of sand grains, (3) chemical composition of interstitial water, and (4) rate of deposition and burial thermal history of the depositional basin (Morad et al. 2010).

Impacts of Porosity-Enhancing Factors

For the studied sequence, the Nubia sandstone is mostly composed of quartz grains with rare relics of feldspars, which may be attributed to dominance of severe dissolution and leaching out of the chemically unstable feldspars during the post-depositional diagenetic history. Alteration of feldspars due to dissolution by invading solutions results in formation of kaolinite as dispersed clay mineral lining and filling the pore spaces as indicated from the petrographic studies (Fig. 4a) as well as the XRD and SEM studies. The leaching out of cement, dissolution and alteration of feldspars increased the inter-granular and intra-granular porosity fraction, which is one of the best types of porosity with high contribution to permeability. The highest inter-granular porosity is assigned to the quartz arenite microfacies in both the Araba and Naqus Formations (RRT1 and RRT2). Therefore, the highest average helium porosity (ϕ_{He}) and permeability (k) values were assigned to both rock types (ϕ_{He} of 18.9% and 24.2%, with k_{av} of 1384.9 md and 1241.0 md, respectively, Table 2). If porosity and permeability values are good to very good, the storage capacity and the flow capacity of the studied sequences are also expected to be good to very good as discussed in the reservoir quality section above. As another contributor to good reservoir quality, microfracturing played additional enhancing role for the Araba and Naqus Formations. They created a subsidiary microfracture system in the highly compacted mudstone facies (RRT4, Fig. 4d), which is composed of very fine to silty-sized angular quartz grains embedded in clayey matrix with more or less parallel lamination (RRT4, Fig. 4d). Despite having the least reservoir quality, some samples have porosities reaching up to 12.2% and fair permeability values (1.67 md).

Impacts of Porosity-Reducing Factors

Cementation, authigenic minerals and mechanical compaction are the dominant porosity-reducing factors in the Nubia sandstone. Cementation is mostly contributed by silica cement in the form of meniscus cement, which has little or no effect on the final porosity net result in the quartz arenite microfacies (RRT1, RRT2). Primary argillaceous material due to deposition in quiet environment is additional matrix cement that dominates in mudstone microfacies causing major reduction in its reservoir quality properties (RRT4). Diagenetic clay minerals are formed as authigenic minerals slightly reducing the porosity and permeability ($\phi_{\text{He}} = 17.1\%$, $k_{\text{av}} = 469$ md, Table 2) of the quartz wacke (RRT3) in the Naqus Formation due to alteration of feldspars into kaolinite booklets filling the pore spaces (Fig. 4f). Therefore, the presence of authigenic kaolinite as dispersed clays, filling the pore spaces, reduced permeability from excellent values ($577 \leq k_{\text{av}} \leq 2224$ md) of the RRT1 and RRT2 samples to good and very good permeability ($46.5 \leq k_{\text{av}} \leq 1267$ md, Table 2) of RRT3 samples.

Gypsum as a subsidiary cement is additional reducing cement material filling the pore channels and fractures of the studied rock types, e.g., RRT1 (Fig. 4e). Due to very good reservoir quality of RRT1 and RRT2 and the low gypsum content (gypsum $\leq 4\%$, Table 1), the effect of gypsum cementation seems to be negligible to slight. This reducing effect increases in the case of RRT3 (quartz wacke microfacies) where gypsum content reaches to 24% and the distribution mode changes from filling pore spaces to poikilotopic cement (Fig. 4c) based on the gypsum content.

Mechanical compaction due to overload pressure is additional reducing effect, which seems to have a little or negligible effect on the reservoir quality of RRT1 and RRT2 samples. The compaction is indicated by the alignment of quartz grains as point contact fabric (Fig. 4a); sometimes suture and concave–convex contact fabrics (Fig. 4b) are an indication of the advance of pressure compaction. The best reservoir quality (RRT1, RRT2) is accompanied by the least pressure compaction (RRT4, Table 2).

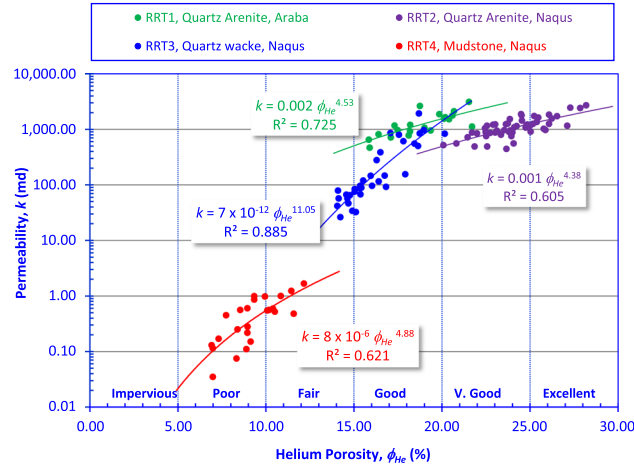


Figure 9. Plots of permeability as a function of porosity measured by helium injection.

Contribution of Porosity (ϕ_{He}) to Permeability (k)

Porosity is one of the main contributors to permeability besides the pore throat diameter and complexity. So, presenting permeability as a function of porosity (Fig. 9) is not always systematic and the output factors of the final model may be a good indication for the pore types and pore throat properties. The output $\phi_{\text{He}}-k$ model indicates similarity of the factor and the porosity exponent between the quartz arenite samples of both the Araba and Naqus Formations indicating similarity in pore types.

$$\text{RRT1} : k = 0.002 \phi_{\text{He}}^{4.53} \quad (R^2 = 0.725) \quad (7)$$

$$\text{RRT2} : k = 0.001 \phi_{\text{He}}^{4.38} \quad (R^2 = 0.605) \quad (8)$$

The relatively moderate coefficient of determination of both equations can be attributed to the presence of different pore types that contribute to the permeability of the different samples. The pore types of the studied quartz arenite of both the Araba and Naqus Formations can be described as intergranular pore spaces and microfractures through the quartz grains (Fig. 4a and c).

Factors of $\phi_{\text{He}}-k$ for the other rock types are completely different from the models obtained for the quartz arenite. The model of the quartz wacke (RRT3) seems to be transitional to that of the mudstone (RRT4) as suggested by the following equations.

$$\text{RRT3} : k = 7 \times 10^{-12} \phi_{\text{He}}^{11.05} \quad (R^2 = 0.885) \quad (9)$$

$$\text{RRT4} : k = 8 \times 10^{-6} \phi_{\text{He}}^{4.88} \quad (R^2 = 0.621) \quad (10)$$

In general, the measured permeability of the studied samples is ranked as fair to very good, whereas the helium porosity is fair to excellent for the studied rock types except for mudstone (RRT4), which is poor to fair (Fig. 9). A general model can be introduced to calculate air permeability of the Cambrian–Ordovician Nubia sandstone sequence in the Gebel El-Zeit area, thus:

$$k = 2 \times 10^{-8} \phi_{\text{He}}^{8.04} \quad (R^2 = 0.891) \quad (11)$$

Impacts of Pore Throat Diameter on Permeability

The mercury injection capillary pressure (MICP) technique is one of the best methods for ranking reservoir rocks (Nabawy and Barakat 2017; Li et al. 2017; Lai et al. 2018a, b).

Pore Throat Distribution Plot

Plotting the pore throat diameter distribution as a function of increasing mercury injection percentage is a helpful descriptive technique for ranking reservoir quality following the ranks published by Nabawy and Barakat (2017) (Table 3). For the present study, four ranks (ranks II, III, IV and V) were established (Fig. 10 and Table 4).

The best rank (II, average mega-pores = 6%, average macro- and mesopores = 82%, Table 4) is

Table 3. Ranking the reservoir quality based on the pore diameter (*D*) distribution obtained from the MICP technique (Nabawy and Barakat 2017)

Pore diameter	Mega-pores ($D \geq 100 \mu\text{m}$)	Macropores ($100 > D \geq 10 \mu\text{m}$)	Mesopores ($10 > D \geq 1.0 \mu\text{m}$)	Micro- and nanopores ($1.0 \mu\text{m} > D$)
Rank I	$P \geq 25\%$		$P \geq 50\%$	$P < 25\%$
Rank II	$P < 25\%$		$P \geq 50\%$	$P < 25\%$
Rank III	–		$P \geq 75\%$	$P < 25\%$
Rank IV	–		$P < 75\%$	$P \geq 25\%$
Rank V	–	–	$P \geq 50\%$	$P < 50\%$
Rank VI	–	–	$P < 50\%$	$P \geq 50\%$

P is the percentage ratio of pore fraction to the total pore volume

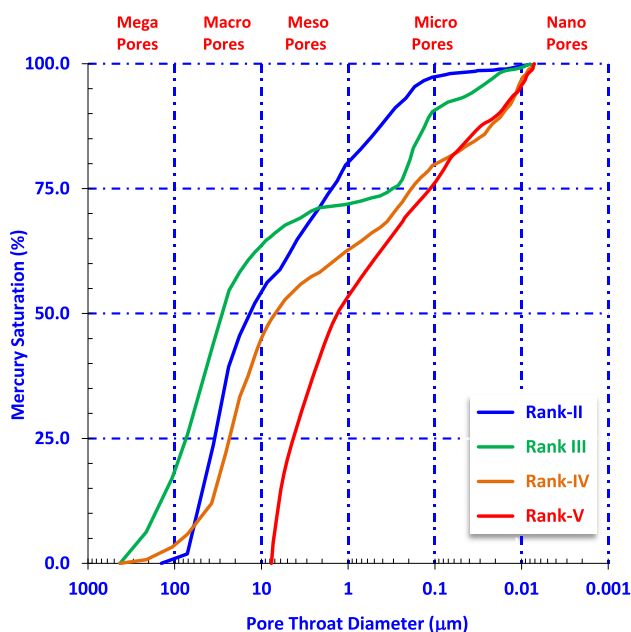


Figure 10. Plots of pore throat diameters obtained from mercury injection capillary pressure (MICP) technique as a function of mercury saturation of the studied rock types.

assigned to the quartz arenite samples from the Naqus Formation, whereas rank III (average macro- and mesopores = 80%, average micro- and nanopores = 20%, Table 4) is assigned mostly to the quartz arenite of the Araba Formation. The least ranks (IV, V) are assigned to both the quartz wacke and mudstone facies, respectively (Fig. 10 and Table 4). The best ranks (II, III) indicates a more or less homogeneous of the pore throat distribution, which is characterized by more than 50% of the pore throat diameters (*D*) in the macrosize ($D \geq 10 \mu\text{m}$) and less than 25% of the pore throat diameters in the range of the micro- and nanosizes (Fig. 10). In contrast, the least ranks refer to heterogeneity of the pore throat distribution with higher percentage of

micro- and nanopore spaces. This heterogeneity may be attributed to the presence of some clay minerals, which are characterized by chaotic distribution through the pore spaces causing slicing and partitioning of the pore spaces into smaller pore spaces (Taghavi et al. 2006; Dutton 2008; Lai et al. 2017a, b, 2018a, b).

Dominance of the micro- and nanopore spaces in RRT4 (mudstone microfacies) is mostly attributed to its silt-sized composition and explains the low reservoir quality of this rock type. In contrast, the good reservoir quality was assigned to the quartz arenite RRT1 and RRT2 samples which is attributed to dominance of macro- and mesopores for these two rock types (Table 4), which are composed

Table 4. Percentages of the different pore throat diameters (D) obtained from MICP tests to the total pore volume

Formation	Lithology	Rank	Mega-pores ($D \geq 100 \mu\text{m}$)	Macropores ($100 > D \geq 10 \mu\text{m}$)	Mesopores ($10 > D \geq 1.0 \mu\text{m}$)	Micro- and nanopores ($1.0 \mu\text{m} > D$)	
Araba Formation	RRT1 (Quartz Arenite)	Min	III	–	76%	15%	
		Average	III	–	80%	20%	
		Max	II	5%	85%	23%	
Naqus Formation	RRT2 (Quartz Arenite)	Min	III	3%	76%	8%	
		Average	II	6%	82%	12%	
		Max	II	10%	89%	19%	
	RRT3 (Quartz Wacke)	Min	V	–	–	57%	34%
		Average	IV	–	–	62%	38%
		Max	IV	–	–	69%	41%
	RRT4 (Mudstone)	Min	V	–	–	51%	36%
		Average	V	–	–	55%	45%
		Max	V	–	–	71%	49%

Ranks and pore sizes are classified following Nabawy and Barakat (2017)

mostly of moderate to very fine quartz grains with relatively low clay content (Fig. 4a and b).

Effective Pore Radius (r_{35} , r_{dp})

The highest average r_{35} (average $r_{35} = 18.79$, $14.39 \mu\text{m}$, macrosizes) and r_{dp} (average $r_{dp} = 24.03$, $18.74 \mu\text{m}$, macrosizes) are assigned to the quartz arenite of both the Naqus and Araba Formations, respectively (Table 2). In contrast, the least pore radii were assigned to the mudstone facies (average $r_{dp} = 0.31$, average $r_{35} = 0.15 \mu\text{m}$, micropores, Table 2).

The effective pore throat radii described as r_{dp} and r_{35} are thought to be the most effective factors governing the permeability values. Plotting average permeability (k_{av}) as a function of pore radii indicates a main dependence of permeability r_{dp} and r_{35} on with very high reliability ($0.942 \geq R^2 \geq 0.739$, Fig. 11). The r_{dp} and r_{35} values of the different rock types indicate macro- to mesopore sizes, but for the mudstone facies they refer to micropore sizes (Fig. 11). Permeability can be calculated as a function of pore throat radii as shown in Figure 11 using similar models for the quartz arenite (RRT1 and RRT2) and quartz wacke facies (RRT3) with a different model for the mudstone facies.

Reservoir Quality Assessment

The reservoir quality assessment depends mostly on storage capacity (porosity, ϕ) and deliverability (permeability, k) of a studied reservoir. It

includes three quality parameters; RQI , NPI and FZI (Amaefule et al. 1993). This quality concept has been tested by many authors through the years (e.g., Tiab and Donaldson 1996; Abbaszadeh et al. 1996; Corbett and Potter 2004; Al-Dhafeeri and Nasr-El-Din 2007; Guo et al. 2007; Teh et al. 2012; Abed 2014; Nabawy and Al-Azazi 2015; El Sharawy and Nabawy 2016a, b; Nabawy and Barakat 2017; Nabawy et al. 2018). For the present study, the quality parameters are estimated based on both helium porosity and average air permeability (k_{av}) to avoid dependence of permeability on direction (Nabawy et al. 2018; El Sharawy and Nabawy 2018). The RQI is mostly dependent on bulk density, porosity and permeability, whereas FZI is based on the same parameters beside RQI but with less reliability than the relationships with RQI . Nabawy et al. (2018) attributed this relatively low reliability to a disturbance raised from the normalized porosity, which depends on both pore and grain phases. For the quartz arenite samples (RRT1 and RRT2), the average RQI values are in the range of mesopore spaces (2.69 , $2.16 \mu\text{m}$, respectively), whereas the average FZI values are in the range of meso- to macrosizes (11.7 , $6.98 \mu\text{m}$, respectively, Table 2). For the mudstone facies (RRT4), the average RQI and FZI values refer to micropore spaces, whereas the quartz wacke samples (RRT3) are characterized by meso- to macropore spaces (1.13 , $5.56 \mu\text{m}$ as average RQI and FZI , respectively).

Reservoir quality assessment is achieved by plotting RQI vs. FZI , which indicates that RRT1 and RRT2 samples have the best quality (Fig. 11). The FZI values for RRT1 are relatively higher than those for RRT2 samples, which may be attributed to

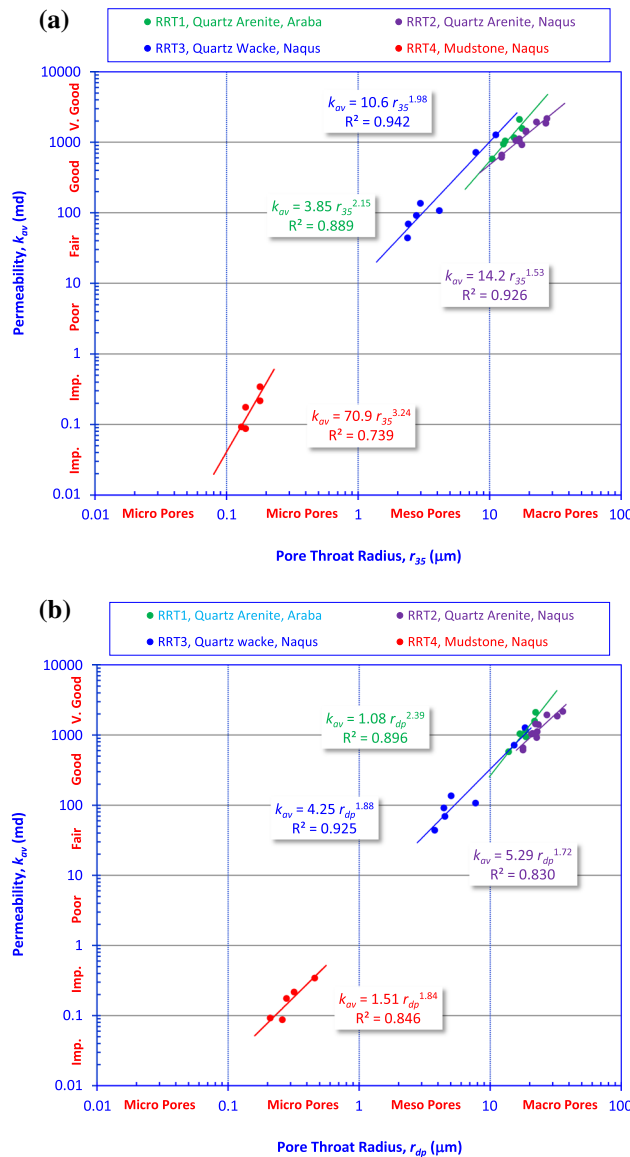


Figure 11. Plots of the pore throat radius of Winland (r_{35} , 1972) and Pittman (r_{dp} , 1992) as a function of the average permeability.

higher average pore sizes rather than the pore throat radii (Table 2). Based on this plot, the quartz wacke facies (RRT3) is considered as fair reservoir whereas the mudstone facies (RRT4) represents impervious streaks within this reservoir (Fig. 12). For more specification, RQI values have been plotted vs. NPI for the different RRTs and discriminated into six hydraulic flow units based on FZI values (Fig. 13). Each HFU represents a group of samples having

similar FZI values, e.g., HFU-4 represents samples that are characterized by $2.5 \leq FZI \leq 5 \mu\text{m}$ (Fig. 13). Therefore, each HFU is limited by two FZI discriminating lines of definite values that were calculated based on the classification introduced by Nabawy and Al-Azazi (2015), El Sharawy and Nabawy (2019). Based on this plot, the studied quartz arenite and wacke samples have fair to very good reservoir properties ($FZI \geq 2.5 \mu\text{m}$), whereas RRT4

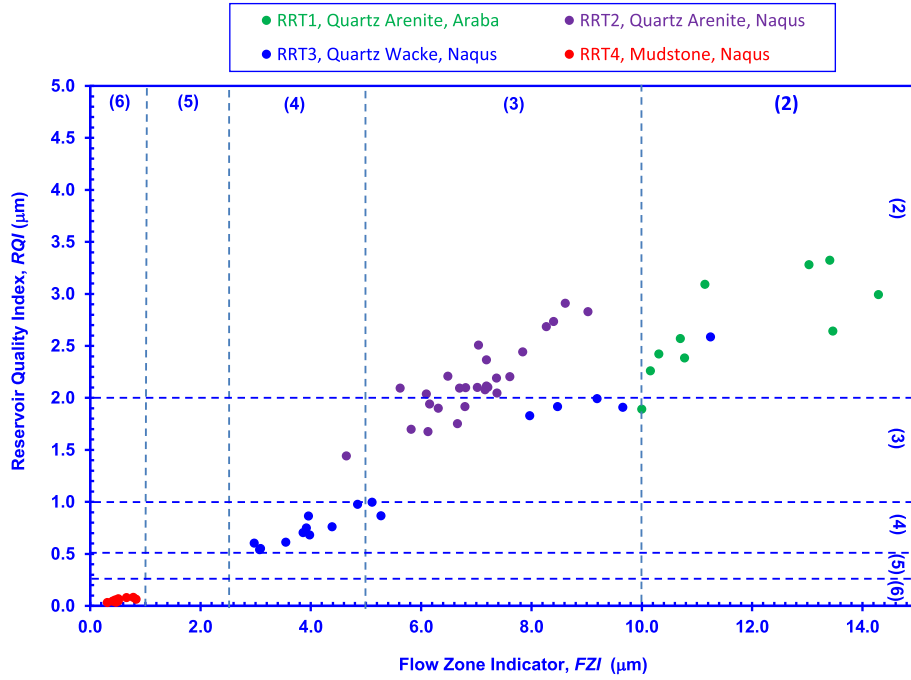


Figure 12. Reservoir quality assessment of the studied rock properties based on *RQI* and *FZI* values. Ranks are based on the quality rank classification proposed by Nabawy and Al-Azazi (2015), Nabawy et al. (2018).

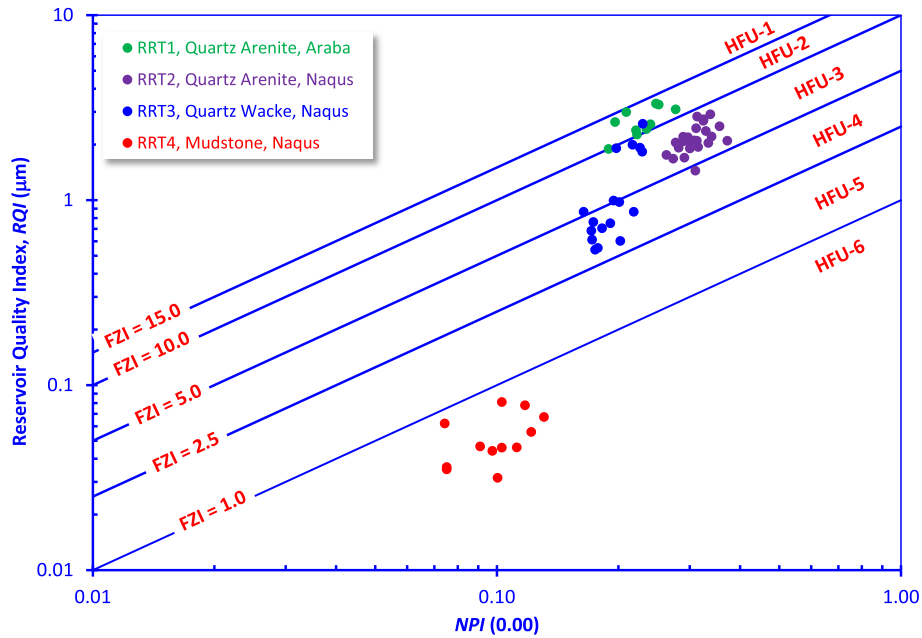


Figure 13. Reservoir quality assessment for the studied rock properties based on *RQI* and *NPI* values. *FZI* values are based on the values proposed by Nabawy and Al-Azazi (2015), Nabawy et al. (2018).

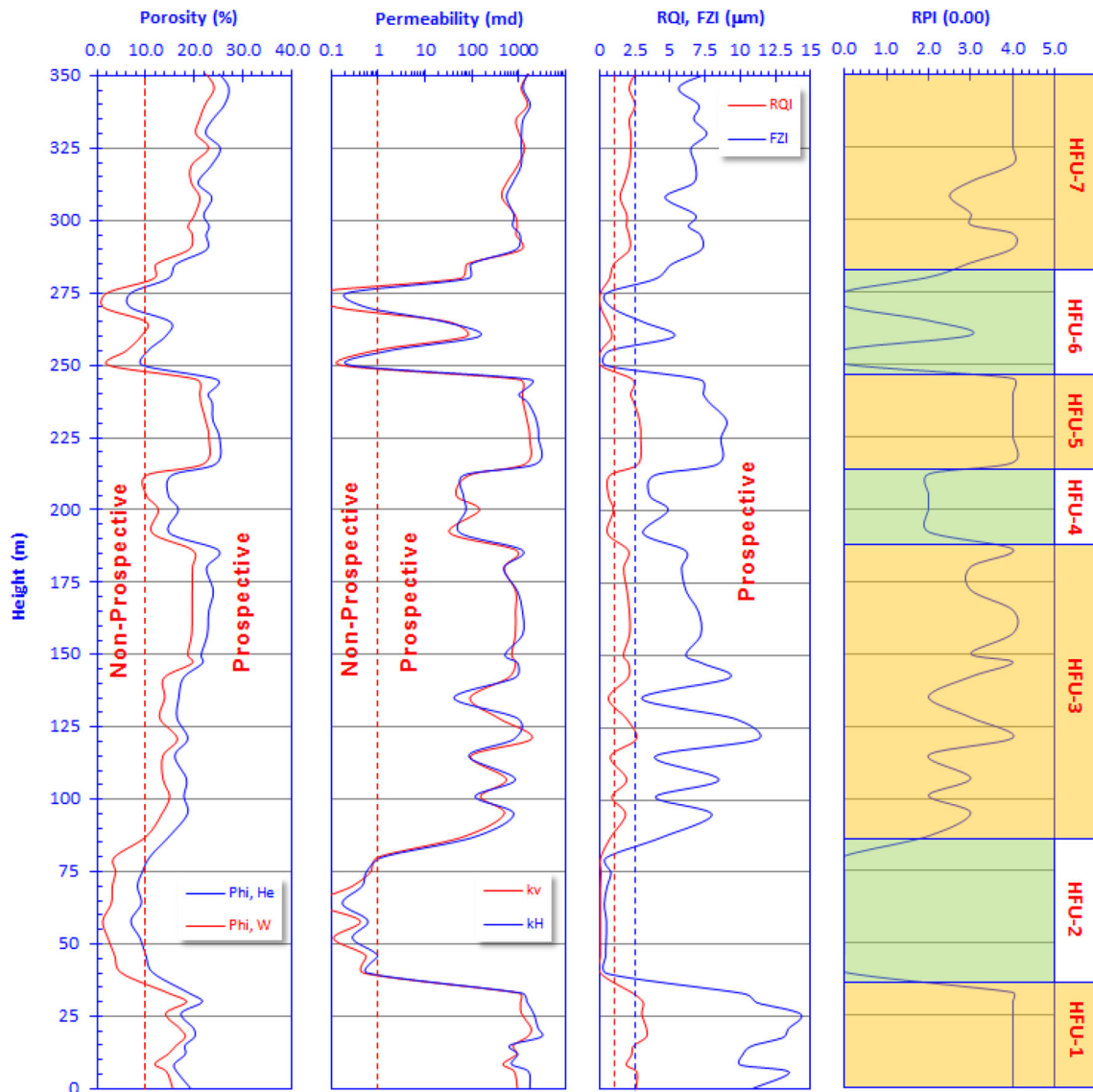


Figure 14. Plots of the petrophysical and reservoir quality parameters as a function of height for the Nubia sandstones in the studied area.

samples are impervious ($FZI \leq 1 \mu\text{m}$) representative of a pressure barrier silty to muddy horizons.

Hydraulic Flow Units (HFUs)

A hydraulic flow unit (HFU) refers to a cumulative thickness of rocks of similar reservoir properties. It can be applied to permeability (k) (Testerman 1962), RQI , FZI , RPI (Nabawy et al. 2018), and can be extended to other reservoir diagnostic parameters. Both the RQI and FZI param-

eters are the net result of statistical processing of both the porosity and permeability. These are the main parameters for characterizing reservoir quality. Due to some differences in rank values, Nabawy and Al-Azazi (2015) also proposed the RPI parameter, which is the mathematical mean of these ranks. Plotting these measured quality parameters (RQI , FZI , RPI) in addition to the water and helium porosities (ϕ_{He} , ϕ_W), air permeability (k_V , k_H), is a successful tool for dividing the studied sequence into HFU zones. For the present study, the Nubia sandstone sequence is divided into seven HFUs, four

potential units intercalated with three non-potential zones (Fig. 14). The HFUs and their potentialities are defined based on some proposed cutoff values, which refer to minimum or maximum threshold values of the required limit to proceed with production ($\phi_{He} \geq 10\%$, $k \geq 1$ md and $RPI \geq 2$). The Araba Formation is mostly represented by HFU-1, which is characterized by fair to good porosity ($\phi_{He} \geq 15\%$). Through the porosity and permeability tracks (first and second tracks) in Figure 14, it is indicated that two zones referred as HFU-2 and HFU-6 (at elevation ranges 40–85 m and 240–285 m) are non-prospective ($\phi_{He} < 10\%$, $k < 1$ md).

The reservoir quality parameters in the *RQI*, *FZI* and *RPI* tracks (third and fourth tracks in Fig. 14) refer to some fluctuation in reservoir quality, in particular through HFU-3 (at elevation range 85–190 m). Though the *RQI* values refer to non-prospective zone (at height 190–215 m), the *FZI* refers to fair quality ($FZI \geq 2.5 \mu\text{m}$), which supports values of the *RPI* ($RPI = 2$, fair quality, Fig. 14). However, this defect in the *RQI* values is declared more clearly by very good permeability values in the permeability track in Figure 14. In addition to this defect, Nabawy et al. (2018) referred to another defect in the *FZI* values due to abnormal contribution to permeability by porosity values in some fractured zones of secondary fabrics. So, conducting the HFU zonation and reservoir quality assessment on *RPI* parameter compensates these defects.

CONCLUSIONS

The integrated studies of petrographic and petrophysical properties are a useful tool for discrimination of the studied sequences into rock types. The studied Cambrian Araba samples in Gebel El-Zeit are described as quartz arenite (RRT1), whereas the Ordovician Naqus Formation is discriminated into three reservoir rock types (RRTs), namely quartz arenite (RRT2), quartz wacke (RRT3) and mudstone (siltstone, RRT4).

Cementation by silica, as meniscus cement and quartz overgrowth, is the main cement material that reduces porosity. Compaction due to overload pressure is additional porosity-reducing diagenetic factor. In contrast, dissolution and leaching out of cement and fracturing are the main porosity-enhancing diagenetic factors. The SEM and XRD studies revealed that kaolinite is the most dominant

authigenic clay mineral that is responsible for reducing porosity and plugging the pore spaces that greatly reduced permeability.

The reservoir quality parameters in addition to the mercury injection capillary pressure (MICP) technique were successfully applied for ranking the storage capacity properties of the studied sequence. The quartz arenite samples from the Araba and Naqus Formations (RRT1, RRT2) are characterized by the best quality, whereas the mudstone is characterized by the least quality.

Presenting the petrophysical properties as a function of depth indicates that the studied sequence can be discriminated into seven HFUs comprised of four highly promising units intercalated with three less promising units.

ACKNOWLEDGMENTS

The authors would like to thank the anonymous reviewers for their significant comments that helped us improve and reconstruct the manuscript. Special thanks are also due to the Editor Prof Dr. John Carranza, whose patience and insightful suggestions have led to a concise revised version. The authors are grateful to the Egyptian General Petroleum Corporation and the Gulf of Suez Petroleum Company for releasing the data.

REFERENCES

- Abbaszadeh, M., Fujii, H., & Fujimoto, F. (1996). Permeability prediction by hydraulic flow units-theory and applications. *Society of Petroleum Engineers, SPE Formation Evaluation SPE-30158-PA*, 11(4), 263–271.
- Abdallah, A. M., & Adindani, A. (1963). Stratigraphy of Upper Paleozoic Rocks, Western Side of the Gulf of Suez. *Geological Survey and Mineral Resource Department, Egypt*, 25, 18.
- Abdallah, A. M., Darwish, M., El Aref, M., & Helba, A. A. (1992a). Lithostratigraphy of the pre-Cenomanian clastics of north Wadi Qena, Eastern Desert, Egypt. In A. Sadek (Ed.), *Proceedings of the first international conference on geology of the Arab World. Cairo University, Cairo* (pp. 255–282).
- Abdallah, A. M., El Aref, M. M., & Helba, A. A. (1992b). Lithostratigraphy of the pre-Cenomanian clastics of north Wadi Qena, Eastern Desert, Egypt. In *Proceedings of 2nd conference geology of the Arab World, Cairo University* (pp. 255–282).
- Abdel-Wahab, A. A. (1988). Lithofacies and diagenesis of the Nubia Formation at Central Eastern Desert, Egypt. In *9th EGPC exploration conference, Cairo* (p. 9).

- Abdel-Wahab, A. A. (1998). Diagenetic history of Cambrian quartz arenite, Ras Dib-Zeit Bay area, Gulf of Suez, Eastern Desert, Egypt. *Sedimentary Geology*, 121(1), 121–140.
- Abed, A. A. (2014). Hydraulic flow units and permeability prediction in a carbonate reservoir, Southern Iraq from well log data using non-parametric correlation. *International Journal of Enhanced Research in Science Technology & Engineering*, 3(1), 480–486.
- Al-Dhafeeri, A. M., & Nasr-El-Din, H. A. (2007). Characteristics of high-permeability zones using core analysis, and production logging data. *Journal of Petroleum Sciences and Engineers*, 55, 18–36.
- Allam, A. (1988). Geological and structural study on Gebel El-Zeit area. *Journal of African Earth Sciences*, 7(7–8), 933–944.
- Amaefule, J. O., Altunbay, M., Tiab, D., Kersey, D. G., & Keelan, D. K. (1993). Enhanced reservoir description: Using core and log data to identify hydraulic (flow) units and predict permeability in uncored intervals/wells. SPE 26436. In *Presented at the annual technical conference and exhibition, Houston, TX* (pp. 3–6).
- Beleity, A. M., Ghoneim, M., Hinawi, M., Fathi, M., Gebali, H., & Kamel, M. (1986). Paleozoic and stratigraphy, paleogeography and paleotectonics in the Gulf of Suez. In *8th EGPC Exploration Conference, Cairo* (pp. 17–23).
- Bhattacharyya, D. P., & Dunn, L. G. (1986). Sedimentological evidence for repeated pre-Cenozoic vertical movements along the northeast margin of the Nubian Craton. *Journal of African Earth Sciences*, 5, 147–153.
- Caputo, M. V., & Crowell, J. C. (1985). Migration of glacial centers across Gondwana during the Phanerozoic Era. *Bulletin of Geological Society of America*, 96, 1020–1036.
- Corbett, P. W. M., & Potter, D. K. (2004). Petrotyping: A base map and Atlas for navigating through permeability and porosity data for reservoir comparison and permeability prediction. In *International symposium of the society of core analysts*.
- David, C., Bertaud, D., Dautriat, J., Sarout, J., Menéndez, B., & Nabawy, B. S. (2015). Detection of moving capillary front in porous rocks using X-ray and ultrasonic methods. *Frontiers in Physics*, 3(A053), 1–14.
- Dutton, S. P. (2008). Calcite cement in Permian deep-water sandstones, Delaware Basin, west Texas: Origin, distribution, and effect on reservoir properties. *AAPG Bulletin*, 92(6), 765–787.
- Eames, L. E. (1984). Palynologic definition of Paleozoic unconformity bounded sequences, Gulf of Suez region, Egypt. In *7th Petroleum exploration and production conference 'EGPC', Cairo* (Vol. 1, pp. 117–125).
- EGPC, Egyptian General Petroleum Corporation. (1996). *Gulf of Suez oil fields: A comprehensive overview*. Cairo: EGPC.
- El Sharawy, M. S., & Nabawy, B. S. (2016a). Determination of electrofacies using wireline logs based on multivariate statistical analysis for the Kareem Formation, Gulf of Suez, Egypt. *Environmental Earth Sciences*, 75(21), 1394.
- El Sharawy, M. S., & Nabawy, B. S. (2016b). Geological and petrophysical characterization of the Lower Senonian Matulla Formation in Southern and Central Gulf of Suez, Egypt. *Arabian Journal for Science and Engineering*, 41(1), 281–300.
- El Sharawy, M. S., & Nabawy, B. S. (2018). Determining the porosity exponent m and lithology factor a for sandstones and their control by overburden pressure: A case study from the Gulf of Suez, Egypt. *AAPG Bulletin*, 102(9), 1893–1910.
- El Sharawy, M. S., & Nabawy, B. S. (2019). Integration of electrofacies and hydraulic flow units to delineate reservoir quality in uncured reservoirs: A case study, Nubia Sandstone Reservoir, Gulf of Suez, Egypt. *Natural Resources Research*. <https://doi.org/10.1007/s11053-018-9447-7>.
- Gazia, M. T. A. (2016). Sedimentological and petrophysical assessment of some of the Gebel El-Zeit Paleozoic Sandstones, Sw Gulf of Suez, Egypt. M.Sc. thesis, Tanta University.
- Guo, G., Diaz, M. A., Paz, F. J., Smalley, J., & Waninger, E. A. (2007). Rock typing as an effective tool for permeability and water-saturation modeling: A case study in a clastic reservoir in the oriente basin. *SPE Reservoir Evaluation & Engineering*, 10(6), 730–739.
- Hassan, A. A. (1967). A new carboniferous occurrence in Abu Durba, Sinai, Egypt. In *6th Arab petroleum Congress 2* (pp. 1–8).
- Ibrahim, A. A. (1996). Petroleum geology of the Cretaceous and pre-Cretaceous sediments in some oil fields in the Gulf of Suez area, Egypt. Unpublished Ph.D. thesis, Cairo University, p. 211.
- Issawi, B., El-Hinnawi, M., Francis, M., & Mazhar, A. (1999). The Phanerozoic geology of Egypt, a geodynamic approach. *Egyptian Geological Survey & Mining Authority, Special Publication*, 76, 462.
- Issawi, B., & Jux, U. (1982). Contributions to the stratigraphy of the Paleozoic rocks in Egypt. *Annals of Geological Survey of Egypt*, 64, 1–28.
- Kassab, M. A. M., Abu Hashish, M., Nabawy, B. S., & El-Nagar, O. (2017). Effect of kaolinite as a key factor controlling the petrophysical properties of the Nubia sandstone in central Eastern Desert, Egypt. *Journal of African Earth Sciences*, 125, 103–117.
- Katz, A. J., & Thompson, A. H. (1987). Prediction of rock electrical conductivity from mercury injection measurements. *Journal of Geophysical Research*, 92, 599–607.
- Khalifa, M., Soliman, H., & Wanas, H. A. (2006). The Cambrian Araba formation in northeastern Egypt: Facies and depositional environments. *Journal of Asian Earth Sciences*, 27, 873–884.
- Klitzsch, E. (1986). Plate tectonics and cratonal geology in Northeast Africa (Egypt/Sudan). *Geologische Rundschau*, 75, 755–775.
- Kolodzie Jr., S. (1980). Analysis of pore throat size and use of the Waxman–Smits equation to determine OOIP in Spindle field. In *55th Annual Fall Technical Conference, SPE 9382*. Colorado: Society of Petroleum Engineers.
- Kora, M. (1984). The Paleozoic outcrops of Um-Bogma area, Sinai, Egypt. Ph.D. thesis, Mansoura University, Mansoura, Egypt, p. 235.
- Lai, J., Wang, G., Chai, Y., Ran, Y., & Zhang, X. (2015). Depositional and diagenetic controls on reservoir pore structure of tight gas sandstones: Evidence from Lower Cretaceous Bashijiqike Formation in Kelasu Thrust Belts, Kuqa Depression in Tarim Basin of West China. *Resource Geology*, 65(2), 55–75.
- Lai, J., Wang, G., Chai, Y., Xin, Y., Wu, Q., Zhang, X., et al. (2017b). Deep burial diagenesis and reservoir quality evolution of high-temperature, high-pressure sandstones: Examples from Lower Cretaceous Bashijiqike Formation in Keshen area, Kuqa depression, Tarim basin of China. *AAPG Bulletin*, 101(6), 829–862.
- Lai, J., Wang, G., Chen, J., Wang, S., Zhou, Z., & Fan, X. (2017a). Origin and distribution of carbonate cement in tight sandstones: The Upper Triassic Yanchang Formation Chang 8 oil layer in west Ordos Basin, China. *Geofluids*, 2017, 8681753.
- Lai, J., Wang, G., Fan, Z., Chen, J., Wang, S., Zhou, Z., et al. (2016). Insight into the pore structure of tight sandstones using NMR and HPMI measurements. *Energy & Fuels*, 30, 10200–10214.
- Lai, J., Wang, G., Wang, S., Cao, J., Li, M., Pang, X., et al. (2018b). Review of diagenetic facies in tight sandstones: Diagenesis, diagenetic minerals, and prediction via well logs. *Earth-Science Reviews*, 185, 234–258.

- Lai, J., Wang, G., Wang, Z., Chen, J., Pang, X., Wang, S., et al. (2018a). A review on pore structure characterization in tight sandstones. *Earth-Science Reviews*, 177, 436–457.
- Li, P., Zheng, M., Bi, H., Wu, S., & Wang, X. (2017). Pore throat structure and fractal characteristics of tight oil sandstone: A case study in the Ordos basin, China. *Journal of Petroleum Science and Engineering*, 149, 665–674.
- Morad, S., Al-Ramadan, K., Ketzer, J. M., & De Ros, L. F. (2010). The impact of diagenesis on the heterogeneity of sandstone reservoirs: A review of the role of depositional facies and sequence stratigraphy. *AAPG Bulletin*, 94(8), 1267–1309.
- Nabawy, B. S. (2015). Impacts of the pore- and petro-fabrics on porosity exponent and lithology factor of Archie's equation for carbonate rocks. *Journal of African Earth Sciences*, 108, 101–114.
- Nabawy, B. S., & Al-Azazi, N. A. S. A. (2015). Reservoir zonation and discrimination using the routine core analyses data: The Upper Jurassic Sab'atayn sandstones as a case study, Sab'atayn basin, Yemen. *Arabian Journal of Geosciences*, 8(8), 5511–5530.
- Nabawy, B. S., & Barakat, M. K. (2017). Formation evaluation using conventional and special core analyses: Belayim Formation as a case study, Gulf of Suez, Egypt. *Arabian Journal of Geosciences*, 10(2), 25, 1–23.
- Nabawy, B. S., & David, C. (2016). X-Ray CT scanning imaging for the Nubia sandstone as a tool for characterizing its capillary properties. *Geosciences Journal*, 20(5), 691–704.
- Nabawy, B. S., & El Sharawy, M. S. (2015). Hydrocarbon potential, structural setting and depositional environments of Hammam Faraun Member of the Belayim Formation, Southern Gulf of Suez, Egypt. *Journal of African Earth Sciences*, 112, 93–110.
- Nabawy, B. S., Rashed, M. A., Mansour, A. S., & Afify, W. S. M. (2018). Petrophysical and microfacies analysis as a tool for reservoir rock typing and modeling: Rudeis Formation, offshore October Oil Field, Sinai. *Marine and Petroleum Geology*, 97, 260–276.
- Nabawy, B. S., & Wassif, N. A. (2017). Effect of the mineralogical composition on the petrophysical behavior of the amygdaloidal and vesicular basalt of Wadi Wizr, Eastern Desert, Egypt. *Journal of African Earth Sciences*, 134, 613–625.
- Nabawy, B. S., & Kassab, M. A. (2014). Porosity-reducing and porosity-enhancing diagenetic factors for some carbonate microfacies: A guide for petrophysical facies discrimination. *Arabian Journal of Geosciences*, 7(11), 4523–4539.
- Pittman, E. D. (1992). Relationship of porosity and permeability to various parameters derived from mercury injection capillary pressure curves for sandstone. *AAPG Bulletin*, 76, 191–198.
- Said, R. (1971). Explanatory note to accompany the geological map of Egypt. *Geological Survey of Egypt*, 56, 123.
- Sakran, Sh, Nabih, M., Henaish, A., & Ziko, A. (2016). Structural regime and its impact on the mechanism and migration pathways of hydrocarbon seepage in the southern Gulf of Suez rift: An approach for finding new unexplored fault blocks. *Marine and Petroleum Geology*, 71, 55–75.
- Salem, A. M. K., Abdel Wahab, A., & McBride, E. F. (1998). Diagenesis of shallow buried cratonic sandstones, southwest Sinai, Egypt. *Sedimentary Geology*, 119, 311–335.
- Schowalter, T. T. (1979). Mechanics of secondary hydrocarbon migration and entrapment. *AAPG Bulletin*, 63(5), 723–760.
- Schütz, K. I. (1994). Structure and stratigraphy of the Gulf of Suez, Egypt. London, S.M. (ed.), Interior Rift Basins. *AAPG Memoir* 59, 57–96.
- Spearing, M., Allen, T., & McAulay, G. (2001). Review of the Winland R35 method for net pay definition and its application in low permeability sands. *International Symposium Proceedings, Society of Core Analysts*, 63, 5.
- Taghavi, A. A., Mørk, A., & Emadi, M. A. (2006). Sequence stratigraphically controlled diagenesis governs reservoir quality in the carbonate Dehloran Field, southwest Iran. *Petroleum Geosciences*, 12, 115–126.
- Teh, W. J., Willhite, G. P., & Doveton, J. H. (2012). Improved reservoir characterization using petrophysical classifiers within electrofacies. In *SPE-154341-PP*.
- Testerman, J. D. (1962). A statistical reservoir-zonation technique. *Journal of Petroleum Technology*, 14(8), 889–893.
- Tiab, D., & Donaldson, E. C. (1996). *Petrophysics, theory and practice of measuring reservoir rock and fluid transport properties* (pp. 205–220). Houston, TX: Gulf Publishing Co.
- Wanas, H. A. (2011). The Lower Paleozoic rock units in Egypt: An overview. *Geoscience Frontiers*, 2(4), 491–507.
- Winland, H. D. (1972). *Oil accumulation in response to pore size changes, Weyburn field, Saskatchewan*. Amaco Production Research Report No. F72-G-25.